


ORIGINAL ARTICLE

Hypoxia-inducible lncRNA MIR210HG interacting with OCT1 is involved in glioblastoma multiforme malignancy

Kuo-Hao Ho^{1,2} | Chwen-Ming Shih^{1,2} | Ann-Jeng Liu³ | Ku-Chung Chen^{1,2} 

¹Graduate Institute of Medical Sciences, College of Medicine, Taipei Medical University, Taipei, Taiwan

²Department of Biochemistry and Molecular Cell Biology, School of Medicine, College of Medicine, Taipei Medical University, Taipei, Taiwan

³Department of Neurosurgery, Taipei City Hospital Ren-Ai Branch, Taipei, Taiwan

Correspondence

Ku-Chung Chen, Department of Biochemistry and Molecular Cell Biology, Taipei Medical University, 250 Wu-Hsing Street, Xinyi District, Taipei 11031, Taiwan.

Email: kuchung@tmu.edu.tw

Funding information

Ministry of Science and Technology, Taiwan, Grant/Award Number: MOST 110-2320-B-038-069; Taipei City Government, Grant/Award Number: 11001-62-022 and 11101-62-030; Taipei City Hospital Ren-Ai, Grant/Award Number: TPCH-110-07

Abstract

An insufficient oxygen supply within the intratumoral environment, also known as hypoxia, induces glioblastoma multiforme (GBM) invasion, stemness, and temozolomide (TMZ) drug resistance. Long noncoding (lnc)RNAs have been reported to be involved in hypoxia and GBM progression. However, their roles in hypoxic GBM malignancy are still unclear. We investigated the mechanisms of hypoxia-mediated lncRNAs in regulating GBM processes. Using The Cancer Genome Atlas (TCGA) and data mining, hypoxia-correlated lncRNAs were identified. A hypoxia-upregulated lncRNA, MIR210HG, locating in nuclear regions, predicted poor prognoses of patients and modulated hypoxia-promoted glioma stemness, TMZ resistance, and invasion. Depletion of hypoxic MIR210HG suppressed GBM and patient-derived cell growth and increased TMZ sensitivity in vitro and vivo. Using RNA sequencing and gene set enrichment analysis (GSEA), MIR210HG-upregulated genes significantly belonged to the targets of octamer transcription factor 1 (OCT1) transcription factor. The direct interaction between OCT1 and MIR210HG was also validated. Two well-established worse prognostic factors of GBM, insulin-like growth factor-binding protein 2 (IGFBP2) and fibroblast growth factor receptor 1 (FGFR1), were identified as downstream targets of OCT1 through MIR210HG mediation in hypoxia. Consequently, the lncRNA MIR210HG is upregulated by hypoxia and interacts with OCT1 for modulating hypoxic GBM, leading to poor prognoses. These findings might provide a better understanding in functions of hypoxia/MIR210HG signaling for regulating GBM malignancy.

KEYWORDS

FGFR1, hypoxic glioblastoma, IGFBP2, MIR210HG, OCT1

Abbreviations: aREA, analytic rank-based enrichment analysis; ASO, antisense oligonucleotide; bFGF, basic fibroblast growth factor; CGGA, chinese glioma genome atlas; DAVID, database for annotation, visualization and integrated discovery; DEG, differentially expressed gene; EGF, epidermal growth factor; FGFR1, fibroblast growth factor receptor 1; GBM, glioblastoma multiforme; GEO, gene expression omnibus; GSC, glioma stem cell; HIF, hypoxia-inducible factor; HIF1A-AS2, HIF-1 α -antisense RNA 2; IDH, isocitrate dehydrogenase; IGF2BP2, insulin-like growth factor-2-binding protein 2; IGFBP2, insulin-like growth factor-binding protein 2; lncRNA, long noncoding RNA; miRNA, microRNA; MTT, 3-(4,5-dimethylthiazol-2-yl)-2,5-diphenyltetrazolium bromide; NF- κ B, nuclear factor κ B; OCT1, octamer transcription factor 1; PDIA3P1, protein disulfide isomerase family A member 3 pseudogene 1; RCI, relative concentration index; RMA, robust multichip average; RNA-Seq, RNA sequencing; shRNA, small hairpin RNA; ssGSEA, single-sample gene set enrichment analysis; TCGA, The Cancer Genome Atlas; TMZ, temozolomide; UCSC, university of california, santa cruz.

This is an open access article under the terms of the Creative Commons Attribution-NonCommercial-NoDerivs License, which permits use and distribution in any medium, provided the original work is properly cited, the use is non-commercial and no modifications or adaptations are made.

© 2021 The Authors. *Cancer Science* published by John Wiley & Sons Australia, Ltd on behalf of Japanese Cancer Association.

1 | INTRODUCTION

Glioblastoma multiforme (GBM), a grade IV glioma, is the most common brain tumor and predominantly occurs in adults.¹ Standard treatments for GBM are a combination of radiation therapy with adjuvant chemotherapeutic temozolomide (TMZ) after maximal surgical resection.² Despite these interventions, the overall survival of GBM patients is only 15-31 months.¹ One of the predominate factors that contributes to malignant features and treatment resistance of GBM is hypoxia. Histologically, pseudopalisading necrosis with surrounding hypoxia is frequently presented in GBM tumor tissues.³ The hypoxic environment induces activation of crucial transcription factors including hypoxia-inducible factor (HIF)-1 α and HIF-2 α , which drive glioma invasion,⁴ angiogenesis, stemness,⁵ and TMZ resistance⁶ through regulating hypoxia-responsive genes. Besides protein coding genes, noncoding RNAs, including micro (mi)RNA and long noncoding (lnc)RNAs, are also recognized as crucial regulators involved in hypoxic glioma malignancy. Although a wide array of miRNAs has been studied in hypoxia-mediated GBM progression,⁷ the roles of lncRNAs in this process are not fully understood.

lncRNAs, noncoding RNAs longer than 200 bp, participate in a wide spectrum of cancer malignancies including drug resistance, cancer stemness, migration, and invasion.⁷⁻⁹ Some lncRNAs have been reported to be involved in hypoxia-promoting glioma progression. Comparing mesenchymal glioma stem cells (GSCs) with proneural GSCs, Mineo et al¹⁰ identified HIF-1 α -antisense RNA 2 (HIF1A-AS2) as a mesenchymal GSC-enriched lncRNA. Mechanistically, HIF1A-AS2 is associated with insulin-like growth factor-2-binding protein 2 (IGF2BP2) and DHX9 to maintain HMGA1 expression, which promotes glioma stemness and survival under hypoxia.¹⁰ Another study took advantage of a microarray of hypoxia-cultured U87-MG glioma cells to identify a hypoxia-induced lncRNA, protein disulfide isomerase family A member 3 pseudogene 1 (PDIA3P1).¹¹ PDIA3P1 functions as a miRNA sponge to inhibit miR-124-3p expression, leading to activation of the nuclear factor (NF)- κ B pathway and mesenchymal transition.¹¹ However, utilization of microarray data to investigate hypoxia-associated lncRNAs might overlook other potential candidates. Thus, we attempted to screen RNA sequencing (RNA-Seq) data of glioma patients to pinpoint crucial hypoxia-associated lncRNAs.

Through in silico analyses of The Cancer Genome Atlas (TCGA) RNA-Seq data, a hypoxia-related lncRNA signature that defined patients with distinct survival was identified. One of the hypoxia-associated lncRNAs, MIR210HG, predicted a poor prognosis and was strongly associated with activated hypoxia signaling across three glioma cohorts. While a study indicated MIR210HG is a potential marker for diagnosing gliomas,¹² few studies explored the molecular functions of MIR210HG in hypoxia-promoting glioma progression. Therefore, in vitro and in vivo experiments were conducted in the present study to delineate the function and role of MIR210HG in hypoxic GBM malignancy.

2 | MATERIALS AND METHODS

2.1 | Chemicals and reagents

U-87 MG, U-118 MG, and patient-derived PDM-123 glioma cells were purchased from the American Type Culture Collection (ATCC). Detailed information on chemicals and reagents is available in Supporting Information.

2.2 | Cell culture, gene transfection, and transduction

U-87 MG and U-118 MG cells were maintained in DMEM containing 10% FBS, 2.5 mmol/L GlutaMAX, 100 units/mL penicillin, and 100 μ g/mL streptomycin. PDM-123 cells were maintained in NeuroCult NS-A basal medium with NS-A proliferation supplement, 20 ng/mL EGF, 20 ng/mL bFGF, and 2 μ g/mL heparin using ultra-low attachment culture dishes. To mimic a hypoxic environment in glioma tissues, glioma cells were cultured in an Eppendorf[®] galaxy[®] 48R CO₂ chamber with 1% O₂. The detailed methods for transfection assays are described in Supporting Information.

2.3 | TCGA, CGGA, and GSE7696 data analysis

To retrieve RNA-Seq data of TCGA (n = 152) and CGGA (n = 693) glioma patients, we respectively queried the Xena UCSC (<https://xena.ucsc.edu/>) and CGGA databases (<http://cgga.org.cn/>). The GSE7696 microarray (n = 80) was downloaded from the GEO database. RNA-Seq data were normalized by RNA-Seq by expectation maximization (RSEM) with log₂ transformation. The microarray-detected gene intensity was normalized by the robust multichip average (RMA) with log₂ transformation. Hypoxia activity was inferred based on hypoxia-induced genes from Hallmark hypoxia using a single-sample gene set enrichment analysis (ssGSEA). To quantify the degree of hypoxia in each tumor tissue from GBM patients, we utilized the hypoxia gene set obtained from the Hallmark database.¹³ A single-sample extension of GSEA was carried out to quantify the hypoxia score.¹⁴ This method allowed us to transform the hypoxia-upregulated gene expression into an enrichment score in each patient. Specifically, the hypoxia-induced genes were rank-normalized based on their expression within a patient. Then, the integral of the empirical cumulative distribution functions (ECDFs) between hypoxia-induced genes and the remaining genes was calculated. The enrichment score was obtained by the difference between the ECDFs of the hypoxia-involved genes and the remaining genes. The algorithm is listed below.

$$P_H^w(H, S, x) = r_j H, jx \leq \sum_{r_j H \in \sum |r_j|^{1/4}} \frac{|r_j|^{1/4}}{\sum |r_j|^{1/4}} \quad (1)$$

$$P_R(H, S, i) = r_j H, ji \leq \sum \frac{1}{(N - N_H)} \quad (2)$$

$$ES(H,S) = \sum_{x=1}^N [P_H^w(H,S,x) - P_R(H,S,x)] \quad (3)$$

For the hypoxia gene signature H of size N_H and single sample S , of the data set of N genes, the genes are ranked according to their expression from high to low: $L = \{r_1, r_2, \dots, r_N\}$. The weighted ECDF of the genes in the hypoxia P_H^w and the remaining gene set P_R are calculated by Equations 1 and 2. The enrichment score $ES(H,S)$ per patient was obtained by Equation 3. Transcription activity of OCT1 in TCGA GBM patients was inferred using an analytic rank-based enrichment analysis (aREA). Briefly, gene expressions of well-annotated and experimentally validated targets of OCT1 derived from Garcia-Alonso et al's¹⁵ study were utilized to calculate OCT1's transcription activity by an aREA. A Pearson correlation analysis was conducted to evaluate associations among hypoxia signaling, OCT1 transcription activity, and MIR210HG, fibroblast growth factor receptor 1 (FGFR1), and insulin-like growth factor-binding protein 2 (IGFBP2) gene expressions. Survival differences among groups were compared by a log-rank test. Raw counts from TCGA GBM RNA-Seq data were used to perform a differentially expressed gene (DEG) analysis to identify hypoxia-correlated lncRNAs via the edgeR package. Unsupervised hierarchical clustering was performed to evaluate whether differentially expressed lncRNAs could define distinct hypoxia groups. The similarity within each patient was evaluated by Pearson's correlation, and Ward's algorithm was applied to cluster glioma patients. Associations between clusters and different hypoxia activity groups were compared by chi-square tests.

2.4 | MIR210HG isoform expression analysis

The detailed methods for isoform analyses are described in Supporting Information.

2.5 | TMZ treatment and cell viability assay

The detailed methods for 3-(4,5-dimethylthiazol-2-yl)-2,5-diphenyltetrazolium bromide (MTT) assays are described in Supporting Information.

2.6 | Immunoblot assays

The detailed methods for immunoblot assays are described in Supporting Information. The quantitative result of each gene is shown below the immunoblotting image.

2.7 | RNA extraction and real-time reverse-transcription quantitative polymerase chain reaction (RT-PCR)

Trizol[®] was utilized to extract total RNA based on the manufacturer's instructions. Cytoplasmic and nuclear RNAs were isolated using

a cytoplasmic and nuclear RNA purification kit (cat. no. 21 000) purchased from NORGEN. The detailed methods for RT-PCR assays are described in Supporting Information (Table S1).

2.8 | Tumor sphere formation assay

The detailed methods for tumor sphere formation assays are described in Supporting Information. After 2 weeks, each diameter from 20 tumor spheres per well were counted for the quantitation.

2.9 | Soft agar colony formation assay

The detailed methods for soft agar colony formation assays are described in Supporting Information.

2.10 | In vivo xenograft study

The in vivo experiments including drug treatment, glioma xenograft establishment, and animal care were approved by the Taipei Medical University Laboratory Animal Care and Use Committee (permit no.: LAC-2019-0114). The procedures strictly followed recommendations in the Guide for the Care and Use of Laboratory Animals of the National Institutes of Health (NIH Publications no. 8023, revised 1978) and ARRIVE guidelines. The detailed methods for in vivo xenograft assays are described in Supporting Information.

2.11 | Immunohistochemistry (IHC)

The detailed methods for IHC assays are described in Supporting Information.

2.12 | Invasion assay

The detailed methods for invasion assays are described in Supporting Information.

2.13 | Next-generation sequencing

The detailed methods for next-generation sequencing are described in Supporting Information.

2.14 | Gene set enrichment analysis (GSEA)

The detailed methods for GSEA are described in Supporting Information.

2.15 | RNA immunoprecipitation (RIP)

RIP was conducted using an EZ-Magna RIP™ RNA-binding protein immunoprecipitation kit (cat. no. 17-701) according to the manufacturer's protocol. The detailed methods for RIP are described in Supporting Information.

2.16 | RNA pulldown assay

The RNA pulldown assay was performed following procedures described in Tsai et al's study.¹⁶ The detailed methods for RNA pulldown assay are described in Supporting Information.

2.17 | Construction of the *IGFBP2* and *FGFR1* promoter reporter plasmids

The detailed methods for constructing plasmids are described in Supporting Information.

2.18 | Chromatin immunoprecipitation (ChIP) assay

ChIP assays were performed according to the manufacturer's instructions (EZ-ChIP™, cat. no. 17-295; Millipore). The detailed methods for ChIP assays are described in Supporting Information.

2.19 | Constructions, RNA pulldown assay, invasion, tumor sphere formation assay, and TMZ treatment of deleted mutants of *MIR210HG*

The detailed methods for constructing deleted mutants and protocols for all assays are described in Supporting Information.

2.20 | Statistical analysis

Data from at least three independent experiments were statistically calculated using Sigma Plot 12.5 (Systat Software) as the mean \pm standard deviation (SD). Significant differences among

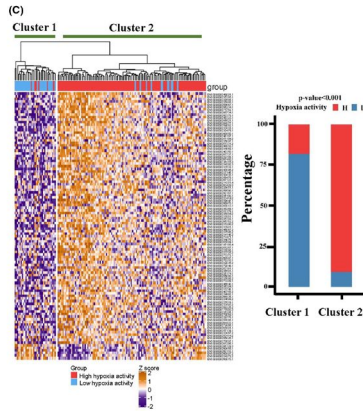
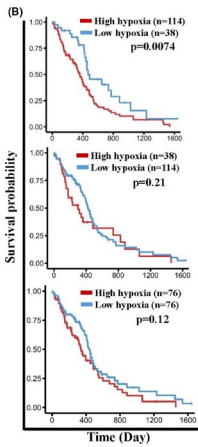
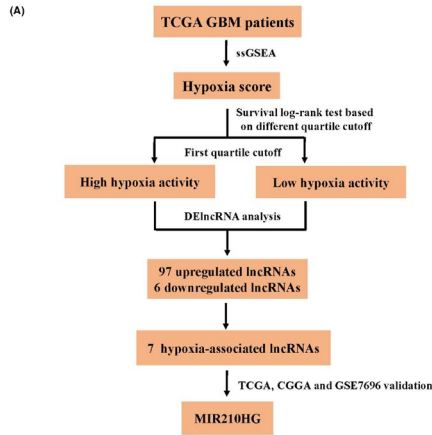
groups were determined using an unpaired *t* test, and $P < .05$ was taken as statistical significance.

3 | RESULTS

3.1 | *LncRNA MIR210HG* is associated with hypoxia and predicts a poor prognosis in GBM patients

We designed a pipeline to identify the critical lncRNAs involved in hypoxic GBM (Figure 1A). To quantify the degree of hypoxia in each patient, transcriptome profiles were analyzed with RNA-Seq data of TCGA GBM patients. An ssGSEA was applied to calculate the hypoxia score based on expression levels of genes derived from Hallmark hypoxia signaling. Higher hypoxic activity predicted a worse GBM prognosis (hazard ratio [HR] = 3.015, $P = .016$). Using different quartile points based on the hypoxia score, GBM patients exhibited significantly different prognosis when divided into two groups based on the first quartile cutoff. (Figure 1B). Thus, using this criterion, the differentially expressed lncRNAs between these two distinct survival groups were identified (Figure 1C, left panel). In total, 97 upregulated and six downregulated lncRNAs (with a false discovery rate [FDR] of <0.01 and absolute multiple of change of >1.5) were found in the high hypoxia activity group (red color) compared with the low one (blue color). To test whether these differentially expressed lncRNAs could distinguish subgroups with different hypoxia activities in TCGA GBM patients, unsupervised hierarchical clustering was performed. Patients were divided into two classes labeled as clusters 1 and 2. Patients with high hypoxia activity were enriched in cluster 2 with a chi-squared P -value of $<.001$ (Figure 1C, right panel), suggesting that this lncRNA signature could identify the patients with high or low hypoxia activity. Furthermore, levels of seven lncRNAs showed significant positive correlations with hypoxia scores (Pearson correlation coefficient $> .5$; P -value $< .001$; Figure 1D). To further pinpoint crucial lncRNAs involved in hypoxic GBM malignancy, candidates were narrowed down according to whether they exhibited a strong correlation with the hypoxia score (Pearson correlation coefficient of $>.6$) and predicted a poor prognosis (log-rank test P -value of $<.01$). Two lncRNAs, *MIR210HG* and *lnc-DLX2-4*, were selected as crucial candidates (Figure 1E and Figure S1). However, only the association of *MIR210HG* with

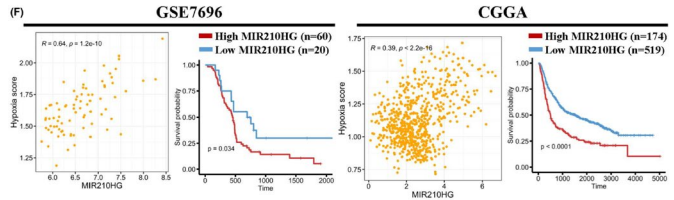
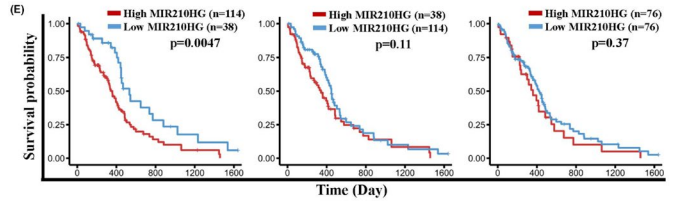
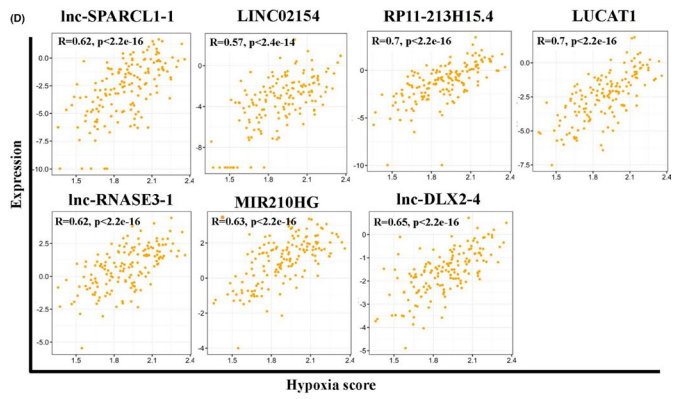
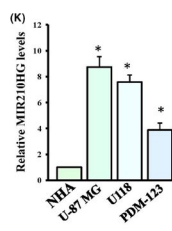
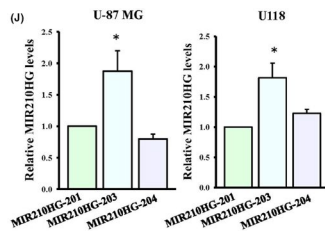
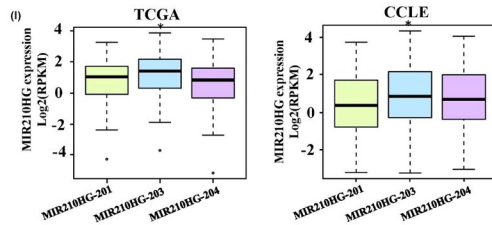
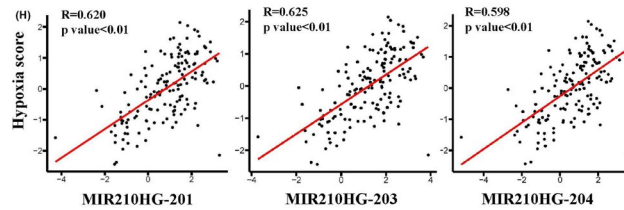
FIGURE 1 *MIR210HG* is significantly associated with hypoxic glioblastoma multiforme (GBM) malignancy and predicts a poor prognosis. A, Flowchart demonstrated the pipeline for identifying the hypoxia-associated and survival-related long noncoding (lnc)RNA candidates. DElncRNA, differentially expressed lncRNAs; ssGSEA, single-sample gene set enrichment analysis. B, Higher hypoxia scores predicted poor prognoses in The Cancer Genome Atlas (TCGA) GBM patients. Different quartile points with log-rank tests were used to categorize patients into different subgroups. C, Heatmap showing differentially expressed lncRNAs between groups with different hypoxic activities. The right panel indicates that patients with high hypoxia activity were enriched in cluster 2. D, Seven lncRNA levels showed significantly positive correlations with hypoxia scores. Higher *MIR210HG* predicted poor prognoses in (E) TCGA GBM patients and was validated with (F) GSE7696 and CGGA data. G, Five *MIR210HG* isoforms are listed in the Ensemble database. H, Three *MIR210HG* isoforms showed significant correlations with hypoxia scores. Higher *MIR210HG*-203 levels were observed in (I) both TCGA and Cancer Cell Line Encyclopedia (CCLE) data, (J) both normoxic U-87 MG and U118 cells, and (K) normoxic tumor cells compared with normal human astrocytes (NHAs). Data are the mean \pm SD of three experiments. * $P < .05$



(G)

Name	Transcript ID	bp	*Flags
MIR210HG-201	ENST00000500447.1	1965	TSL.2
MIR210HG-203	ENST00000533920.1	816	TSL.2
MIR210HG-202	ENST00000528245.1	639	TSL.3
MIR210HG-204	ENST00000534540.1	367	TSL.2
MIR210HG-205	ENST00000665964.1	1962	

*TSL annotations:
 TSL 2 – the best supporting mRNA is flagged as suspect or the support is from multiple expressed sequence tags (ESTs).
 TSL 3 – the only support is from a single EST.



poor survival could be validated using two other independent datasets, GSE7696 and CGGA (Figure 1F). Next, we further evaluated whether MIR210HG expression levels in patients were correlated with clinical backgrounds (Figure S2), MIR210HG levels were higher in tumor versus normal tissues, IDH wild type versus mutation, and mesenchymal versus other subtypes, but not correlate with age and gender using TCGA data. Thus, we focused on the role of MIR210HG in hypoxic GBM progression.

To identify the principal isoform of MIR210HG, the Ensemble database was queried.¹⁷ In total, five isoforms of MIR210HG have been described. Among these isoforms, MIR210HG-201, MIR210HG-203, and MIR210HG-204 belong to transcript support level 2 (TSL2), indicating that multiple expressed sequence tags (ESTs) support their existence (Figure 1G). These three isoforms all exhibited strong positive associations with the hypoxia score, especially MIR210HG-203 (Figure 1H). To further investigate expression levels of these three isoforms in TCGA GBM patients and in glioma cells of the Cancer Cell Line Encyclopedia (CCLE), MIR210HG-203 was the most abundantly expressed isoform (Figure 1I). This finding was also validated with U-87 MG and U118 cells (Figure 1J). The normoxic endogenous levels of MIR210HG were also measured with normal human astrocyte (NHA), U-87 MG, U118, and patient-derived PDM-123 cells. Higher levels of MIR210HG existed in GBM cells compared with NHA cells (Figure 1K). Thus, we mainly focused on MIR210HG-203 for overexpression and knockdown experiments in the present study.

3.2 | MIR210HG is involved in hypoxia-mediated GBM malignancy

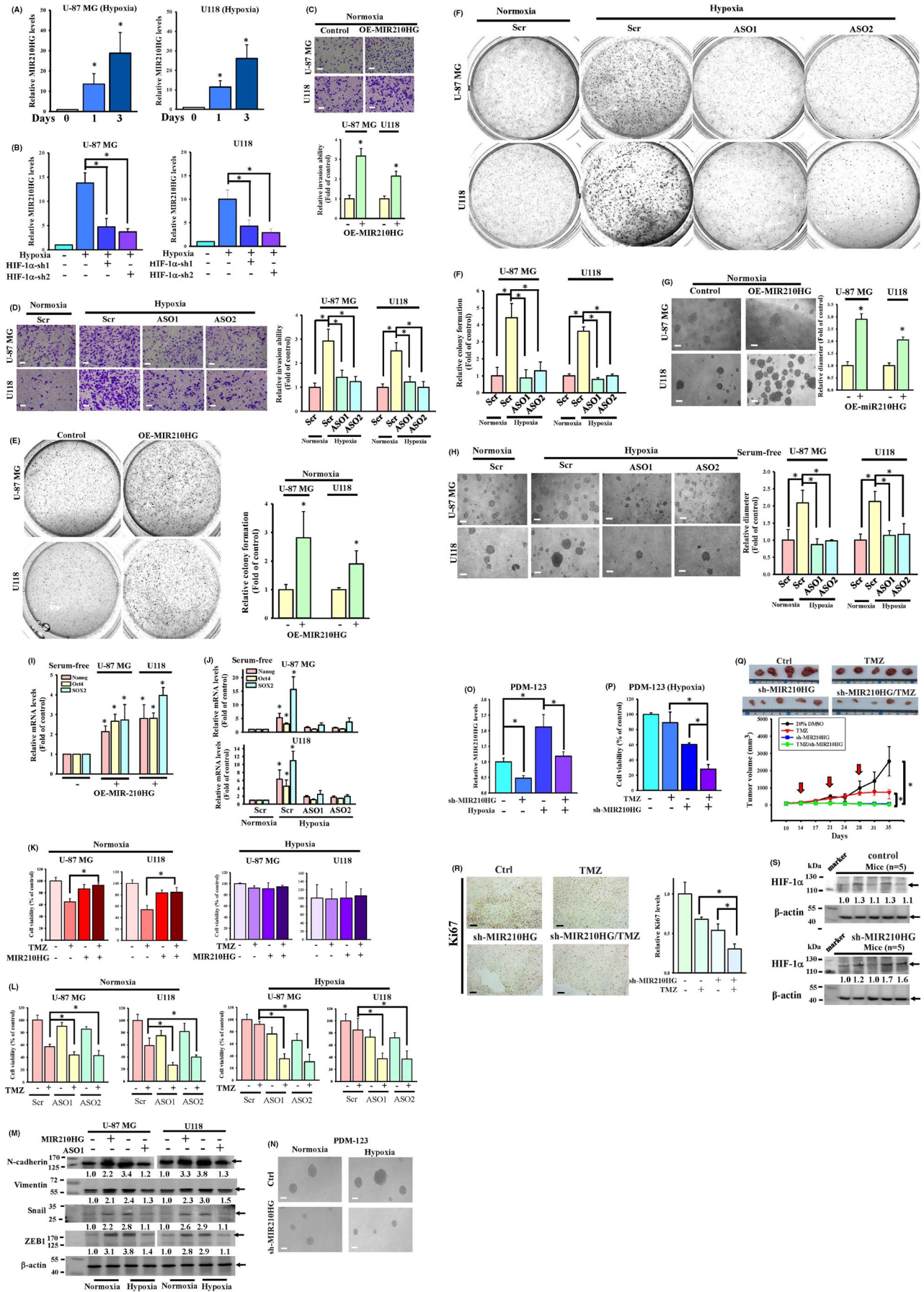
Endogenous MIR210HG expression was significantly upregulated in 1% hypoxia-incubated GBM cells (Figure 2A) and downregulated after HIF-1 α depletions (Figure 2B), suggesting that MIR210HG gene expression was dramatically enhanced by HIF-1 α signaling from normoxia to hypoxic environment. Then, overexpression of MIR210HG in normoxia or MIR210HG depletion in hypoxia with ASOs was respectively used to monitor the functions of MIR210HG in GBM malignancy. MIR210HG overexpression in normoxia significantly enhanced endogenous MIR210HG levels, leading to higher glioma invasion, increasing colony formation and

sphere generation, elevating cancer stemness gene expressions with serum-free cultured GBM cells, inducing TMZ resistance, and upregulating epithelial-to-mesenchymal transition (EMT) marker expressions (Figure 2C-M and Figure S3). By contrast, MIR210HG depletion in hypoxia with ASOs significantly reduced these effects. Depletion of MIR210HG in hypoxia-incubated patient-derived PDM-123 cells also reduced sphere formation (Figure 2N) and hypoxia-induced MIR210HG levels (Figure 2O), and enhanced TMZ cytotoxicity (Figure 2P). Using xenograft experiments with MIR210HG small hairpin RNA (shRNA) stably expressing U-87 MG cells, depletion of MIR210HG significantly reduced the tumor volume and demonstrated a better response to TMZ treatment compared with the controls in vivo (Figure 2Q). By detecting Ki67 and HIF-1 α levels, MIR210HG-depleted U-87 MG cells had slower proliferation rates compared with the controls in hypoxic environments (Figure 2R,S). These results suggest that hypoxia-inducible MIR210HG significantly promoted glioma malignancy.

3.3 | OCT1 is involved in hypoxia/MIR210HG-promoted GBM malignancy

To explore MIR210HG-related genes, protein-coding genes correlated with MIR210HG expression in TCGA GBM patients were calculated. Totally, 1336 genes exhibited significant positive correlations with MIR210HG, and these genes were further divided into hypoxia-associated and non-hypoxia-associated genes. Significantly more positive correlations were observed between MIR210HG and hypoxia-associated genes than with non-hypoxia-associated genes (Figure 3A), suggesting that MIR210HG-related genes are enriched in hypoxia signaling. Additionally, an RNA-Seq analysis with MIR210HG-overexpressing U-87 MG cells was conducted (Figure 3B). Overall, 1702 gene candidates were found to be significantly upregulated (File S1). Combining data from MIR210HG-related genes in TCGA GBM patients and upregulated genes in the RNA-Seq analysis, 142 crucial candidates promoted by MIR210HG were selected (Figure 3C and File S2). Using GSEA, these 142 genes were found to be enriched in cancer malignancy-related pathways, such as phosphatidylinositol 3-kinase (PI3K)/Akt signaling, and focal adhesion (Figure 3D and Table S2).

FIGURE 2 MIR210HG is involved in hypoxic glioblastoma multiforme (GBM) malignancy. A, MIR210HG expression was upregulated with 1% hypoxia incubation. B, The knockdown effects of HIF-1 α on hypoxia-upregulated MIR210HG expression. MIR210HG levels were measured using real-time PCR assays. Data are the mean \pm SD of three experiments. * P < .05. Overexpression in normoxia and knockdown with antisense oligonucleotides (ASOs) in hypoxia of MIR210HG influenced GBM cell invasion (C and D), colony formation (E and D), sphere formation (G and H), cancer stemness with serum-free cultured cells (I and J), temozolomide (TMZ) resistance (K and L), and epithelial-to-mesenchymal transition (EMT) marker expressions (M). Data are the mean \pm SD of three experiments. * P < .05. The knockdown effects of MIR-210HG on sphere formation (N), hypoxia-induced MIR210HG expression (O), and TMZ cytotoxicity (P) in patient-derived PDM-123 cells. Knockdown of MIR210HG in xenograft mice models reduced tumor volume and growth curves (Q) and Ki67 (R) levels and enhanced TMZ cytotoxicity. * P < .05. Red arrows mean the TMZ treatment days. S, The hypoxia-inducible factor (HIF)-1 α levels in mice tissues. Scale bar: 100 μ m. The values below the immunoblotting image are the quantitative results compared with control group



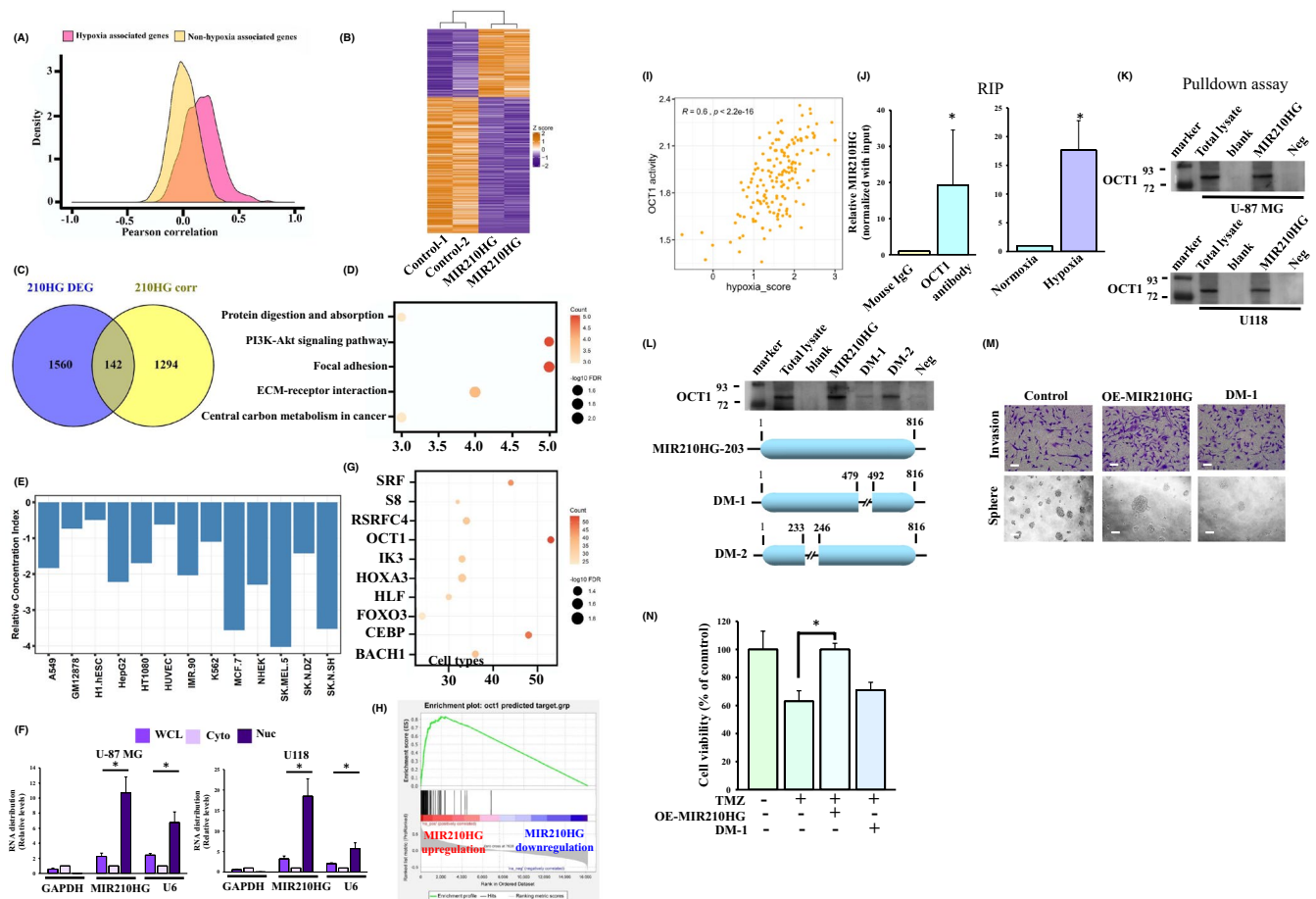


FIGURE 3 MIR210HG interacts with octamer transcription factor 1 (OCT1). A, The density plots demonstrated the distribution of correlation coefficient between MIR210HG and hypoxia/non-hypoxia-associated genes. Kolmogorov-Smirnov test was performed to evaluate the differences of these two distributions. The y-axis represented the probability density function for the kernel density estimation. The x-axis represented the Pearson correlation coefficients between MIR210HG and hypoxia/non-hypoxia-associated genes. B, Heatmap showing the differentially expressed genes in MIR210HG-overexpressed U-87MG compared with empty vector-transfected U-87MG using RNA-sequencing analyses. C, A Venn diagram demonstrated that 142 genes were upregulated and highly correlated with MIR210HG expression in The Cancer Genome Atlas (TCGA) glioblastoma multiforme (GBM) patients. D, Dot plots demonstrated the MIR210HG-regulated genes-enriched top signaling. The x-axis represented the fold enrichment for each pathway. The color depth for each dot indicated the number of genes that mapped to the indicated signaling. The size of each dot represented the values of negative log₁₀-transformed false discovery rate (FDR). E, MIR210HG was mainly distributed in nuclear regions of different cells according to IncALTAS analyses. The y-axis represents the relative concentration index (RCI) values. A negative value indicated that the MR210HG expression was more abundant in nucleus compared with cytoplasm. F, Cellular distributions of MIR210HG identified using nuclear and cytosolic fractionation assays. Data are the mean \pm SD of three experiments. * $P < .05$. G, Putative transcription factors enriched in 142 candidate gene promoters predicted using DAVID analyses. H, MIR210HG-upregulated genes enriched in OCT1-predicted targets. I, OCT1 activity was positively associated with hypoxia scores in GBM patients. OCT1 was identified to interact with MIR210HG using (J) pull-down and (K) RNA immunoprecipitation (RIP) assays. DM-1 mutant showed lower OCT1-binding activity using pull-down assays (L), reducing invasion and sphere formation (M), and no effects on temozolomide (TMZ) cytotoxicity (N). * $P < .05$. For the RNA pull-down assay, OCT1 antibody was used to detect the enrichment of Oct1 after pulling down the RNA protein complex. The schematic in (L) showed the deleted sites of OCT1-binding locations in MIR210HG, respectively named as DM-1 and DM-2. Scale bar means 100 μ m

It is well established that the intracellular distribution decides the physiological functions of an lncRNA. According to the IncALTAS, the relative concentration index of MIR210HG in several cell lines is less than zero (Figure 3E), suggesting that MIR210HG is mainly expressed in nuclei. To further quantify intracellularly distributed levels of MIR210HG, after cellular fractionation, GAPDH and U6 were respectively used as markers for cytoplasmic and nucleus regions. MIR210HG expression was significantly enriched in the nuclear

region (Figure 3F). Because MIR210HG was mainly located in nuclei, we hypothesized that MIR210HG might be associated with transcription factors regulating gene transcription. Thus, transcription factors enriched in 142 MIR210HG-promoted genes were analyzed using DAVID functional annotation tools (Figure 3G). OCT1 was identified as the top transcription factor. Overall, promoter regions of 53 MIR210HG-regulated genes contained predicted OCT1-binding sites (Table S3). Using a GSEA, MIR210HG-upregulated genes were

positively correlated with OCT1-predicted targets (Figure 3H). In addition, OCT1 transcription activity was positively associated with the hypoxia score (Figure 3I). Two putative binding sites were predicted in the MIR210HG-203 sequence using the TFBIND website (Figure S4A). Through performing RIP assays, enriched MIR210HG levels were found to be immune-precipitated using OCT1 antibodies (Figure 3J). Moreover, hypoxia enhanced the association between MIR210HG and OCT1 compared with the normoxia group. RNA pull-down assays demonstrated that OCT1 was coprecipitated with an *in vitro*-transcribed biotinylated MIR210HG transcript (Figure 3K). Then, two OCT1-binding site-deleted MIR210HG mutants, respectively named as DM-1 and DM-2, were synthesized and used to further confirm the interaction between MIR210HG and OCT1 (Figure S4B). Only DM-1 reduced the ability to bind with OCT1 using RNA pulldown assays (Figure 3L). Further, comparing with wild type MIR210HG, overexpression of DM-1 did not show significantly positive effects on enhancing cell invasion (Figure 3M), increasing sphere formation (Figure 3M), and reducing TMZ cytotoxicity (Figure 3N). Finally, to confirm the roles of OCT1 in hypoxia/MIR210HG axis-promoted glioma malignancy, cell invasion (Figure 4A), colony formation (Figure 4B), and sphere formation assays (Figure 4C) were conducted and stemness marker expression (Figure 4D), TMZ treatment responses (Figure 4E), and EMT marker expressions (Figure 4F) were measured. OCT1 depletion prevented MIR210HG-promoted GBM malignancy in normoxia and also reduced hypoxia-enhanced glioma progression. Consequently, MIR210HG associating with OCT1 participated in hypoxia-regulated GBM progression.

3.4 | MIR210HG/OCT1 signaling regulates FGFR1 and IGFBP2 expressions in hypoxia

To explore the relationships between MIR210HG and OCT1, the endogenous OCT1 mRNA and protein levels in MIR210HG-overexpressing and -depleted cells were measured. Neither MIR210HG overexpression nor knockdown of MIR210HG affected OCT1 mRNA and protein levels (Figure S5). Thus, we speculated that MIR210HG might regulate OCT1 transcriptional activities but not enhance OCT1 gene expression. To investigate the roles of MIR210HG in mediating OCT1 transcriptional regulation, we focused on gene candidates that were upregulated in MIR210HG-overexpressing cells and also belonged to OCT1 targets. Through survival analyses, 16 survival-associated candidates were identified. Among these candidates, IGFBP2 and FGFR1 were reported to be highly involved in GBM malignancy. Thus, we tested whether the MIR210HG/OCT1 axis could regulate these two genes in the hypoxic GBM process. First, GBM patients with higher levels of these two genes exhibited poor survival (Figure 5A and Figure S6). Positive correlations were also observed between these two genes and hypoxia scores or OCT1 activities (Figure 5B). MIR210HG overexpression increased IGFBP2 and FGFR1 gene expressions and protein levels in normoxia (Figure 5C,D). By contrast, OCT1 knockdown significantly attenuated MIR210HG-upregulated IGFBP2 and FGFR1 levels. Moreover,

hypoxia-promoted FGFR1 and IGFBP2 levels were decreased after MIR210HG or OCT1 depletion (Figure 5E,F), suggesting that FGFR1 and IGFBP2 were upregulated through the MIR210HG/OCT1 axis in hypoxic GBM.

Using JASPAR predictions,¹⁸ two and one putative OCT1-binding sites were respectively located in FGFR1 and IGFBP2 gene promoters (Figure 5G). To further confirm whether the effects of MIR210HG on FGFR1 and IGFBP2 levels were transcriptionally regulated by OCT1, promoter reporter assays and ChIP-qPCR analyses were respectively performed. MIR210HG overexpression in normoxia enhanced both IGFBP2 and FGFR1 promoter activities, but inhibition of OCT1 suppressed these effects (Figure 5H). Hypoxia-induced IGFBP2 and FGFR1 promoter activities were respectively reduced after knockdown of MIR210HG or OCT1 (Figure 5I). Associations of OCT1 with promoter regions of IGFBP2 and FGFR1 increased in normoxic MIR-210HG-overexpressing cells according to the ChIP-qPCR results (Figure 5J). Incidentally, only the F2 site in FGFR1 promoter regions was the main binding region of OCT1. Depletion of MIR210HG decreased hypoxia-enhanced associations of OCT1 with promoter regions of IGFBP2 and FGFR1 using ChIP-qPCR (Figure 5K). Expression levels of these two genes also decreased in MIR210HG-depleted cells compared with the controls *in vivo* (Figure 5L-N), suggesting that hypoxia-induced MIR210HG enhanced OCT1-regulating downstream genes in GBM malignancy.

4 | DISCUSSION

Emerging research has highlighted the prominent impacts of lncRNA regulation in hypoxia-promoted cancer malignancies. The first evidence demonstrating the potential roles of lncRNAs in response to hypoxia was reported by Choudhry et al.¹⁹ They performed an RNA-Seq assay combined with ChIP-Seq to uncover various lncRNAs involved in HIF-1 α - and HIF-2 α -mediated transcriptions in hypoxic conditions.¹⁹ In gliomas, different approaches have also been taken to pinpoint hypoxia-mediated lncRNAs. Microarray screening with hypoxia-cultured glioma cells revealed an lncRNA, PDIA3P1, involved in the mesenchymal transition.¹¹ An RNA-Seq analysis of exosomes derived from hypoxia-cultured glioma stem cells identified that linc01060 maintains c-Myc transcription activity through translocating MZF1 into nuclei.²⁰ However, few studies explored clinically important hypoxia-associated lncRNAs in glioma patients. The present study analyzed GBM RNA-Seq data from TCGA, and 103 lncRNAs showed tight associations with hypoxia activation. Prominently, these hypoxia-associated lncRNAs defined glioma patients with distinct survival. Among the hypoxia-associated lncRNAs, MIR210HG was found to be upregulated by hypoxia and indicated poor prognoses in TCGA, CGGA, and GSE7696 data.

MIR210HG is transcribed from the ENSG00000247095.2 gene, which is located on chromosome 11p15.5. The intron region of MIR210HG contains the primary form of miR-210. Although miR-210 is a well-characterized hypoxia-induced miRNA²¹ and plays crucial roles in glioma malignancy,²²⁻²⁴ few studies have explored

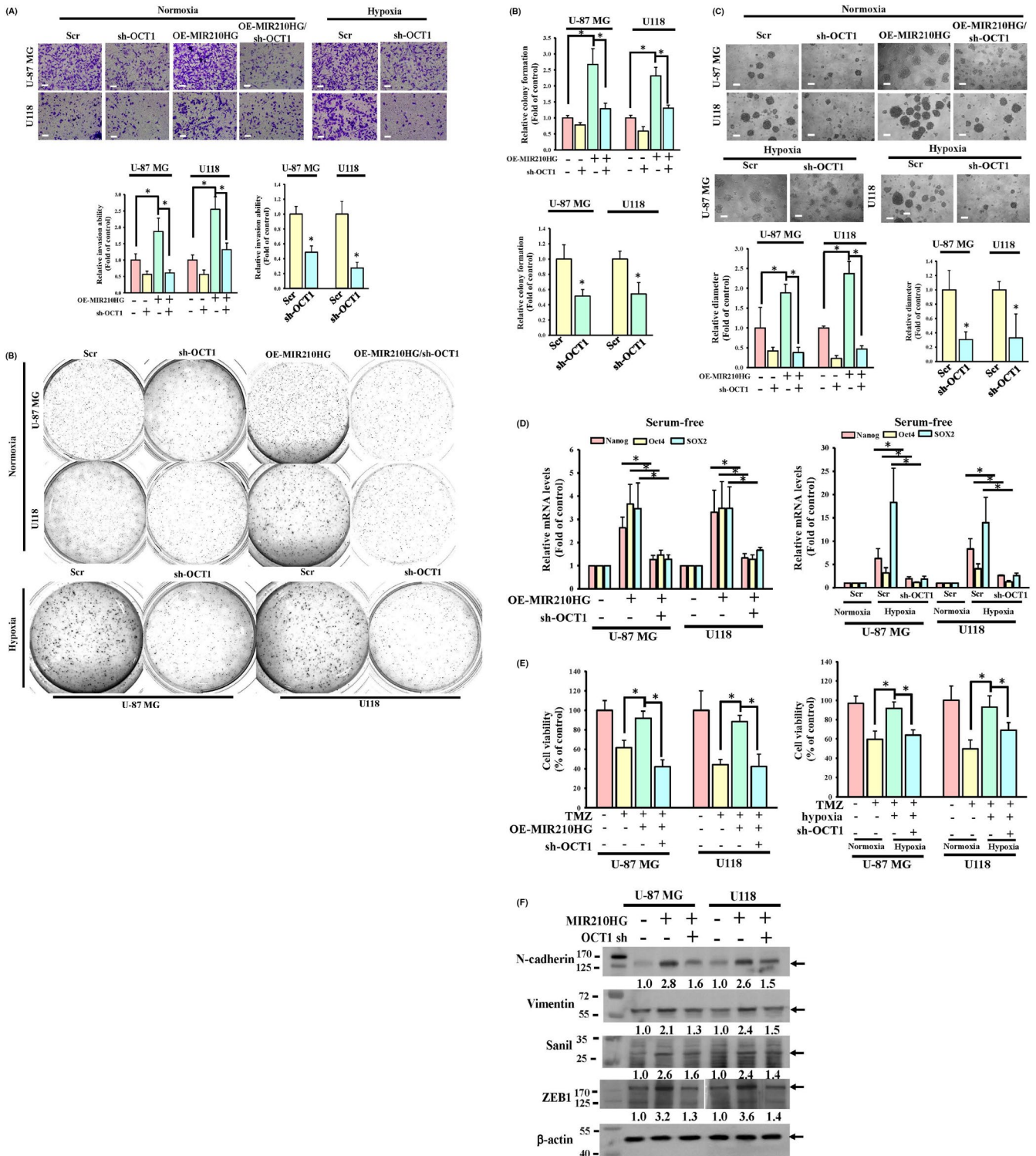


FIGURE 4 Knockdown of octamer transcription factor 1 (OCT1) significantly attenuates MIR210HG-regulated hypoxic GBM malignancy. Knockdown of OCT1 reduced normoxic MIR210HG-regulated and hypoxia-enhanced glioblastoma multiforme (GBM) cell invasion (A), colony formation (B), sphere formation (C), cancer stemness (D), temozolomide (TMZ) resistance (E), and epithelial-to-mesenchymal transition (EMT) marker expressions (F). Data are the mean ± SD of three experiments. *P < .05. Scale bar: 100 μm. The values below the immunoblotting image are the quantitative results compared with control group

the function of MIR210HG in hypoxia-mediated glioma progression. The present study demonstrated that MIR210HG is a hypoxia-inducible lncRNA, and its expression is positively associated with

hypoxia activity in glioma patients. From a literature review, it was reported that MIR210HG is upregulated in glioma tissues.¹² In addition, MIR210HG was identified as regulating the EMT in non-small

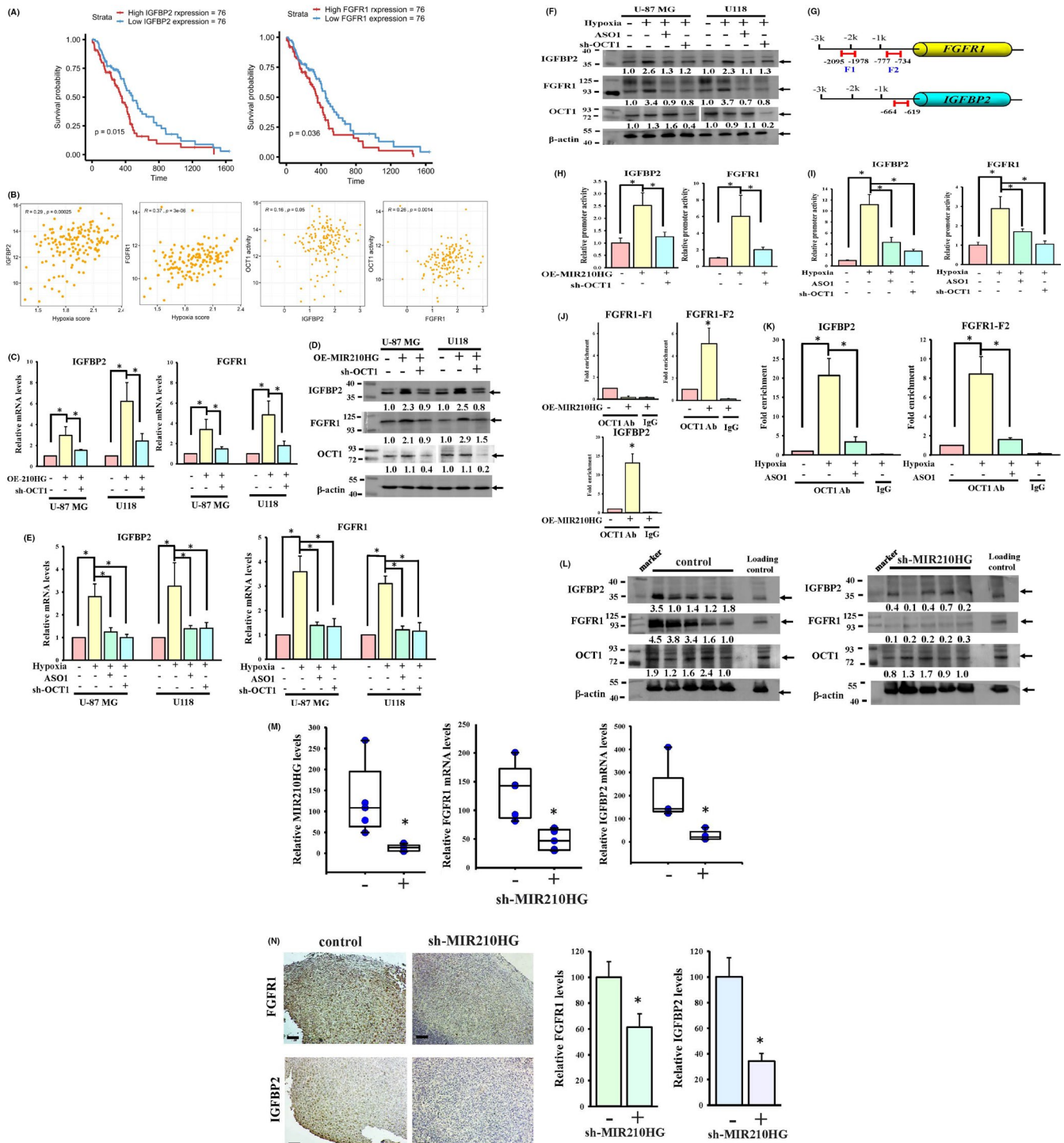


FIGURE 5 MIR210HG is involved in expressions of octamer transcription factor 1 (OCT1)-regulated genes, insulin-like growth factor-binding protein 2 (IGFBP2), and fibroblast growth factor receptor 1 (FGFR1). A, Log-rank tests indicated that higher IGFBP2 and FGFR1 expressions both predicted poor prognoses in The Cancer Genome Atlas (TCGA) glioblastoma multiforme (GBM) patients. B, IGFBP2 and FGFR1 were respectively positively correlated with hypoxia scores and OCT1 activities in GBM. C-F, mRNA and protein levels of IGFBP2 and FGFR1 were regulated by the hypoxia/MIR210HG/OCT1 axis. mRNA and protein levels of IGFBP2 and FGFR1 were respectively measured using real-time PCR and immunoblotting assays. Data are the mean \pm SD of three experiments. * P < .05. G, Predicted OCT1-binding sites located in promoter regions of IGFBP2 and FGFR1 using JASPAR. H-K, Promoter activities of IGFBP2 and FGFR1 were regulated by the hypoxia/MIR210HG/OCT1 axis. Promoter reporter assays (H and I) and ChIP-qPCR (J and K) were respectively conducted. Data are the mean \pm SD of three experiments. * P < .05. L-N, The protein and mRNA levels of IGFBP2 and FGFR1 were reduced in the MIR210HG-knockdown group of mice. mRNA and protein levels were respectively measured using a real-time PCR, immunoblotting, and immunohistochemistry (IHC) assays. One of the control groups was obtained from our preliminary experiment. Data are the mean \pm SD of three experiments. * P < .05. Scale bar: 100 μ m. The values below the immunoblotting image are the quantitative results compared with control group

cell lung cancer²⁵ and osteosarcomas.²⁶ However, a direct link between MIR210HG and the mesenchymal transition as well as other malignant features in glioma have not been confirmed until now. By analyzing RNA-Seq data from MIR210HG-overexpressing U-87 MG cells and TCGA GBM patients, we showed that MIR210HG-regulated genes were enriched in pathways related to the mesenchymal transition, including PI3K/AKT, focal adhesion, and extracellular matrix interactions. Functionally, MIR210HG was identified to be involved in hypoxia-promoted anchorage-independent growth, stemness, invasion, and TMZ resistance in glioma cells. These findings suggest that MIR210HG is a crucial lncRNA participating in hypoxia-mediated glioma malignancy.

OCT1 belongs to the Pit-Oct-Unc (Pit1, Oct1/2, Unc86) family and shares similar *in vitro* DNA-binding specificity with its other family members.²⁷ It was shown that OCT1 maintains stem cell functions in normal cells as well as tumor cells.²⁸ OCT1 target genes, namely *Abcg2*, *Abcb1*, *Abcb4*, and *Aldh1a1*, are associated with stem cell properties.²⁸ Further, OCT1 downregulation decreases the frequencies of tumor-initiating cells in breast and colon cancers.²⁸ OCT1 was also respectively linked to EMT activation and treatment resistance in breast and prostate cancers.^{29,30} However, the functions of OCT1 in gliomas are still unclear. In our present study, OCT1 gene expression did not increase with hypoxia. However, MIR210HG was identified to be associated with OCT1 in nuclei. Moreover, the association between MIR210HG and OCT1 increased with hypoxia, which augmented OCT1's transcription activity of regulating expressions of its targets. Functionally, OCT1 depletion attenuated MIR210HG- and hypoxia-promoted glioma malignancy. Intriguingly, another study identified a different mechanism that enhanced OCT1's transcription activity upon hypoxia. They demonstrated that PER2, which assembles repressor complexes at the promoter region of the OCT1-binding site, was degraded under hypoxia.²⁹ This leads to enhanced transcription of OCT1 downstream targets, including TWIST1 and Slug, in breast cancer stem cells.²⁹ Given these findings, OCT1's transcription activity is increased through various mechanisms in cancers under hypoxia. In the future, a comprehensive ChIP-Seq analysis with an antibody against OCT1 upon hypoxia is needed to further understand its roles in hypoxia-mediated glioma progression.

Considerable evidence has confirmed the oncogenic roles of FGFR1 and IGFBP2. FGFR1, a receptor tyrosine kinase, recognizes fibroblast growth factors, leading to receptor dimerization.³¹ Subsequently, intracellular receptor domains of FGFR1 are phosphorylated, which activates downstream effector molecules.³¹ FGFR1 signaling promotes glioma malignancy *in vivo* by increasing expressions of the stem cell transcription factors SOX2, OLIG2, and ZEB.³² The AKT/mitogen-activated protein kinase (MAPK) and RAC1/CDC42 pathways are also promoted by FGFR1 signaling in inducing glioma proliferation and migration.³³ IGFBP2, a secreted protein, interacts with IGFs to promote IGF-regulated pathways.³⁴ IGFBP2 is highly expressed in 80% of glioma tissues and identified as a significant prognostic marker in glioma patients.³⁵ IGFBP2 was linked to increasing migration, invasion, and TMZ resistance through interacting with integrin $\beta 1$ in gliomas.³⁶ Additionally, IGFBP2

coordinately regulates growth factors such as PDGFB to sustain glioma malignancy.³⁷ However, few studies indicate the roles of IGFBP2 and FGFR1 in glioma under hypoxia. We demonstrated that FGFR1 and IGFBP2 expressions were promoted by hypoxia/MIR210HG/OCT1 signaling, which provides a novel regulatory mechanism that contributes to aberrant expressions of these two oncogenes.

In summary, MIR210HG was identified as a crucial hypoxia-regulated lncRNA that predicts poor prognosis and participates in hypoxia-mediated glioma invasion, cancer stemness, and TMZ resistance. MIR210HG is significantly associated with the OCT1 transcription factor. Mechanistically, MIR210HG was also identified to promote the transcription activity of OCT1, regulating expressions of the oncogenes IGFBP2 and FGFR1. These findings shed light on the development of novel mechanisms for GBM in the future.

ACKNOWLEDGMENTS

This study was sponsored by the Ministry of Science and Technology, Taiwan (contract grant no. MOST 110-2320-B-038-069 to Ku-Chung Chen), Taipei City Government (contract grant no. 11001-62-022 and 11101-62-030 to Ann-Jeng Liu), and Taipei City Hospital Ren-Ai Branch (contract grant no. TPCH-110-07 to Ann-Jeng Liu). We also thank the National RNAi Core Facility at Academia Sinica, Taiwan for providing shRNA reagents and related services and acknowledge the Laboratory Animal Center at Taipei Medical University for the *in vivo* xenograft experiments.

ORCID

Ku-Chung Chen  <https://orcid.org/0000-0002-4696-3924>

REFERENCES

- Louis DN, Perry A, Reifenberger G, et al. The 2016 world health organization classification of tumors of the central nervous system: a summary. *Acta Neuropathol.* 2016;131:803-820.
- Davis ME. Glioblastoma: overview of disease and treatment. *Clin J Oncol Nurs.* 2016;20:S2-S8.
- Brat DJ, Castellano-Sanchez AA, Hunter SB, et al. Pseudopalisades in glioblastoma are hypoxic, express extracellular matrix proteases, and are formed by an actively migrating cell population. *Cancer Res.* 2004;64:920-927.
- Méndez O, Zavadil J, Esencay M, et al. Knock down of HIF-1 α in glioma cells reduces migration *in vitro* and invasion *in vivo* and impairs their ability to form tumor spheres. *Mol Cancer.* 2010;9:133.
- Li Z, Bao S, Wu Q, et al. Hypoxia-inducible factors regulate tumorigenic capacity of glioma stem cells. *Cancer Cell.* 2009;15:501-513.
- Pistollato F, Abbadi S, Rampazzo E, et al. Intratumoral hypoxic gradient drives stem cells distribution and MGMT expression in glioblastoma. *Stem Cells.* 2010;28:851-862.
- Agrawal R, Pandey P, Jha P, Dwivedi V, Sarkar C, Kulshreshtha R. Hypoxic signature of microRNAs in glioblastoma: insights from small RNA deep sequencing. *BMC Genom.* 2014;15:686.
- Gutschner T, Diederichs S. The hallmarks of cancer: a long non-coding RNA point of view. *RNA Biol.* 2012;9:703-719.
- Spizzo R, Almeida MI, Colombatti A, Calin GA. Long non-coding RNAs and cancer: a new frontier of translational research? *Oncogene.* 2012;31:4577-4587.
- Mineo M, Ricklefs F, Rooj A, et al. The long non-coding RNA HIF1A-AS2 facilitates the maintenance of mesenchymal glioblastoma stem-like cells in hypoxic niches. *Cell Rep.* 2016;15:2500-2509.

11. Wang S, Qi Y, Gao X, et al. Hypoxia-induced lncRNA PDIA3P1 promotes mesenchymal transition via sponging of miR-124-3p in glioma. *Cell Death Dis.* 2020;11:168.
12. Min W, Dai D, Wang J, et al. Long noncoding RNA miR210HG as a potential biomarker for the diagnosis of glioma. *PLoS One.* 2016;11:e0160451.
13. Liberzon A, Birger C, Thorvaldsdóttir H, Ghandi M, Mesirov JP, Tamayo P. The molecular signatures database (MSigDB) hallmark gene set collection. *Cell Syst.* 2015;1:417-425.
14. Barbie DA, Tamayo P, Boehm JS, et al. Systematic RNA interference reveals that oncogenic KRAS-driven cancers require TBK1. *Nature.* 2009;462:108-112.
15. Garcia-Alonso L, Iorio F, Matchan A, et al. Transcription factor activities enhance markers of drug sensitivity in cancer. *Cancer Res.* 2018;78:769-780.
16. Tsai M-C, Manor O, Wan Y, et al. Long noncoding RNA as modular scaffold of histone modification complexes. *Science.* 2010;329:689-693.
17. Cunningham F, Achuthan P, Akanni W, et al. Ensembl 2019. *Nucleic Acids Res.* 2019;47:D745-D751.
18. Fornes O, Castro-Mondragon JA, Khan A, et al. JASPAR 2020: update of the open-access database of transcription factor binding profiles. *Nucleic Acids Res.* 2020;48:D87-D92.
19. Choudhry H, Schödel J, Oikonomopoulos S, et al. Extensive regulation of the non-coding transcriptome by hypoxia: role of HIF in releasing paused RNAPol2. *EMBO Rep.* 2014;15:70-76.
20. Li J, Liao T, Liu H, et al. Hypoxic glioma stem cell-derived exosomes containing linc01060 promote progression of glioma by regulating the MZF1/c-Myc/HIF-1 α . *Cancer Res.* 2021;81:114-128.
21. Huang X, Ding L, Bennewith KL, et al. Hypoxia-inducible miR-210 regulates normoxic gene expression involved in tumor initiation. *Mol Cell.* 2009;35:856-867.
22. Yang W, Wei J, Guo T, Shen Y, Liu F. Knockdown of miR-210 decreases hypoxic glioma stem cells stemness and radioresistance. *Exp Cell Res.* 2014;326:22-35.
23. Lai N-S, Wu D-G, Fang X-G, et al. Serum microRNA-210 as a potential noninvasive biomarker for the diagnosis and prognosis of glioma. *Br J Cancer.* 2015;112:1241-1246.
24. Agrawal R, Garg A, Benny Malgulwar P, Sharma V, Sarkar C, Kulshreshtha R. p53 and miR-210 regulated NeuroD2, a neuronal basic helix-loop-helix transcription factor, is downregulated in glioblastoma patients and functions as a tumor suppressor under hypoxic microenvironment. *Int J Cancer.* 2018;142:1817-1828.
25. Kang X, Kong F, Huang K, et al. lncRNA MIR210HG promotes proliferation and invasion of non-small cell lung cancer by upregulating methylation of CACNA2D2 promoter via binding to DNMT1. *Oncotargets Ther.* 2019;12:3779-3790.
26. Li J, Wu QM, Wang XQ, Zhang CQ. Long noncoding RNA miR210HG sponges miR-503 to facilitate osteosarcoma cell invasion and metastasis. *DNA Cell Biol.* 2017;36:1117-1125.
27. Herr W, Sturm RA, Clerc RG, et al. The POU domain: a large conserved region in the mammalian pit-1, oct-1, oct-2, and *Caenorhabditis elegans* unc-86 gene products. *Genes Dev.* 1988;2:1513-1516.
28. Maddox J, Shakya A, South S, et al. Transcription factor Oct1 is a somatic and cancer stem cell determinant. *PLoS Genet.* 2012;8:e1003048.
29. Hwang-Verslues WW, Chang P-H, Jeng Y-M, et al. Loss of corepressor PER2 under hypoxia up-regulates OCT1-mediated EMT gene expression and enhances tumor malignancy. *Proc Natl Acad Sci USA.* 2013;110:12331-12336.
30. Obinata D, Takayama K, Fujiwara K, et al. Targeting Oct1 genomic function inhibits androgen receptor signaling and castration-resistant prostate cancer growth. *Oncogene.* 2016;35:6350-6358.
31. Itoh N, Terachi T, Ohta M, Seo MK. The complete amino acid sequence of the shorter form of human basic fibroblast growth factor receptor deduced from its cDNA. *Biochem Biophys Res Commun.* 1990;169:680-685.
32. Hale JS, Jimenez-Pascual A, Kordowski A, et al. ADAMDEC1 maintains a novel growth factor signaling loop in cancer stem cells. *bioRxiv.* 2019: 531509.
33. Fukai J, Yokote H, Yamanaka R, Arao T, Nishio K, Itakura T. EphA4 promotes cell proliferation and migration through a novel EphA4-FGFR1 signaling pathway in the human glioma U251 cell line. *Mol Cancer Ther.* 2008;7:2768-2778.
34. Baxter RC. Insulin-like growth factor (IGF)-binding proteins: interactions with IGFs and intrinsic bioactivities. *Am J Physiol Endocrinol Metab.* 2000;278:E967-E976.
35. Fuller GN, Rhee CH, Hess KR, et al. Reactivation of insulin-like growth factor binding protein 2 expression in glioblastoma multiforme: a revelation by parallel gene expression profiling. *Cancer Res.* 1999;59:4228-4232.
36. Han S, Li Z, Master LM, Master ZW, Wu A. Exogenous IGFBP-2 promotes proliferation, invasion, and chemoresistance to temozolomide in glioma cells via the integrin β 1-ERK pathway. *Br J Cancer.* 2014;111:1400-1409.
37. Dunlap SM, Celestino J, Wang H, et al. Insulin-like growth factor binding protein 2 promotes glioma development and progression. *Proc Natl Acad Sci USA.* 2007;104:11736-11741.

SUPPORTING INFORMATION

Additional supporting information may be found in the online version of the article at the publisher's website.

How to cite this article: Ho K-H, Shih C-M, Liu A-J, Chen K-C. Hypoxia-inducible lncRNA MIR210HG interacting with OCT1 is involved in glioblastoma multiforme malignancy. *Cancer Sci.* 2022;113:540-552. doi:[10.1111/cas.15240](https://doi.org/10.1111/cas.15240)